# Modelling reflooding of intact core geometries in ASTEC V2.1: Improvements and validation on PERICLES experiments

Laurent Laborde, Ignacio Gomez Garcia Torano

# Modelling reflooding of intact core geometries in ASTEC V2.1: improvements and validation on PERICLES experiments

## Authors and affiliations:

*Ignacio Gómez-García-Toraño, Laurent Laborde**

Institut de Radioprotection et de Sûreté Nucléaire, Service des Accidents Majeurs (SAM)

BP 3 - 13 115 Saint Paul lez Durance Cedex, France

*corresponding author (email: laurent.laborde@irsn.fr, phone: +33 442 19 95 16)

## Abstract

The injection of water into core is a key Accident Management strategy in water-cooled nuclear reactors. Among the flow regimes implicated during reflooding, the most significant one in terms of heat transfer removal is the transition boiling. This mechanism takes place over a short distance near the quench front, which is difficult to capture when using coarse meshes, typically in integral severe accident codes. In the ASTEC V2.1 integral severe accident code, the user can select among two concurrent two-phase thermalhydraulics modelling (five- or six-equation scheme) and for each one, two alternative reflooding models to describe transition boiling region (TBR). On one hand, the DROPLET model calculates a large heat transfer coefficient over a user-defined distance above the quench front. On the other hand, the EXPCHF model calculates the heat flux downstream by imposing the Critical Heat Flux at the quench front and prescribing an exponentially decreasing heat flux along a flow-dependent length.

This article aims at selecting the most appropriate reflooding model for the evaluation of the heat transfer associated with transition boiling in ASTEC V2.1 both for the five and the six-equation hydrodynamic model. For that purpose, experimental data from the PERICLES facility dealing with the reflooding of intact core geometries have been used.

After an exhaustive analysis of the different reflooding models and hydrodynamic models, this study has found that the DROPLET model should be selected when using the five-equation scheme, since it provides enough rod precooling above the quench front. However, the EXPCHF model should be selected when using the six-equation scheme, since it benefits from the larger amount of liquid available near the front. This last configuration gives the best results on the simulated PERICLES tests and is thus recommended for reactor applications.

## Highlights

- ASTEC V2.1 reflooding model for rod-like geometries is validated against PERICLES facility.
- DROPLET reflooding alone is recommended for the five-equation scheme.
- EXPCHF reflooding model is recommended for the six-equation scheme.

## Nomenclature

Acronyms:

- CHF: Critical Heat Flux
- IQF: quench front mesh
- PCT: Peak Cladding Temperature
- QF: Quench front
- SAMG: Severe Accident Management Guidelines
- ZQF: quench front elevation

General variables:

- $C_1$: constant associated with the calculation of $L_l$ (m)
- Ca: Capillary number (-)
- $f_{int}(\bar{\alpha})$: interfacial friction factor in the six-equation scheme (kg/m$^4$)
- $F(\bar{\alpha})$: smoothing function for drift calculation in the five-equation scheme (-)
- $F^{adv}$: advection term (Pa/m)
- $F^{grav}$: hydrostatic pressure gradient (Pa/m)
- $F^{reg}$: regular friction term (Pa/m)
- $F^{sing}$: singular friction term (Pa/m)
- $F_{LG}^{int}$: interfacial friction between the gas and liquid phases in the six-equation scheme (Pa/m)
- $F_{NR}$ : non-stratified interfacial friction term in the five-equation scheme (kg/m$^4$)
- g: gravity (m/s$^2$)
- $H_D$: heat transfer coefficient to the DROPLET model (W/m$^2$K)
- *I*: inertia term (Pa/m)
- $L_l$: characteristic length of the TBR associated with the EXPCHF model (m)
- *Re*: Reynolds number (-)
- $T_{BO}$: burnout temperature (K)
- $T_{liq}$: liquid temperature (K)
- $T_{MFB}$: minimum film boiling temperature (K)
- $T_{sat}$: saturation temperature (K)
- $T_{wall}$: wall temperature (K)
- $v_G$, $v_L$: gas, liquid velocity (K)
- Z: elevation (m)
- $Z_D$: characteristic height associated to the DROPLET model (m)

Greek letters:

- $\alpha$: void fraction (-)
- $\alpha_D$: threshold void fraction associated to the DROPLET model (-)
- $\Delta V = v_G - v_L$: drift velocity (m/s)
- $\varphi_{TBR}^{i}$: heat transfer along the TBR using the *i* reflooding model (W/m$^2$)
- $\mu_k$: dynamic viscosity (Pa s)
- $\rho_k$: density (kg/m$^3$)
- $\sigma_k$: surface tension (N/m)

Subscripts, superscripts:

- G: gas phase
- i: reflooding model (DROPLET or EXPCHF)
- J: junction under consideration
- L: liquid phase
- W: wall
- M: mixture between L and G
- Sat: saturation

# 1 Introduction

The injection of water into the core, frequently called core reflooding, is one of the prime Accident Management strategies in all current Light Water Reactors (Hermsmeyer et al., 2014). Reflooding starts at any time after the Reactor Control Protection System switches on the Emergency Core Cooling System. The action prevents core degradation if launched before the Core Exit Temperature exceeds a given threshold, generally 650ºC corresponding to Peak Cladding Temperatures of about 950ºC (NEA-OECD, 2010). Beyond that limit, the focus of the actions shifts towards the mitigation of the accident, ranging from the core damage minimization to prevention of vessel failure. Thus, reflooding is considered as one of the most important thermal-hydraulic phenomena in the context of nuclear safety. As a matter of fact, this mechanism allowed the mitigation of the severe accident at Three Miles Island Unit 2, despite the core underwent significant degradation (Broughton et al., 1989).

Considerable experimental efforts have been invested over the last decades to study the heat transfer mechanisms taking place within the core during reflooding. Rod bundle reflooding experiments at the FLECHT-SEASET (Lee et al., 1982), FEBA (Ihle and Rust, 1984), PERICLES (Digonnet and Veteau, 1989; Housiadas et al., 1989) and the RBHT (Hochreiter et al., 2012) facilities have contributed to enhance the understanding on such mechanisms for intact core geometries using a wide range of thermal-hydraulic conditions (e.g. system pressure, injection flow rate, initial temperature, inlet subcooling, power). Likewise, rod bundle reflooding experiments at the LOFT FP-2 (Cronenberg, 1992), CORA (Schanz et al., 1992) and QUENCH (Sepold et al., 2001; Steinbrück et al., 2010) facilities have contributed to the same goal for partially degraded cores under low pressures, both conditions being representative of a reflooding scenario during the early in-vessel phase of a severe accident. As a matter of fact, a thorough analyses of the latter experiments contributed to identify criteria for the successful coolability of partially degraded cores (Hering et al., 2015; Hering and Homann, 2007).

Visual studies representative of sub-channel of an intact core performed by (Ishii and De Jarlais, 1987; Obot and Ishii, 1988) have shown that the governing heat transfer regimes occurring during reflooding can be split in nuclear boiling (upstream the quench front), transition boiling (just above the quench front) and dispersed film boiling (well above the quench front). Of special importance is the Transition Boiling Region (TBR), which covers a length of up to few centimetres along which there is a non-stable two-phase flow leading to large heat exchanges with the wall. This length depends on the existing flow regimes above the quench front, which depend on the void fraction at the quench front (linked to the pressure, inlet subcooling, residual power and flow rate). Low system pressures, low flow rates and/or high residual powers lead to a significant increase of the void fraction as soon as the flow at the quench front becomes saturated, the flow above the front ending up being highly dispersed (Yadigaroglu et al., 1993) and the TBR becoming increasingly shorter. A sketch of these experimental observations is depicted at the centre of Figure 1, the depiction of flow patterns being inspired in the figure from (Nelson and Unal, 1992).

The modelling of reflooding is a challenging task not only for severe accident codes, but also for best-estimate system thermalhydraulic codes like CATHARE (France), ATHLET (Germany), TRACE and RELAP5 (USA) or MARS (Korea), as evidenced in the BEMUSE benchmark (Mendizábal et al., 2017). As far as the modelling in integral severe accident codes is concerned, the main challenge is to model the significant heat transfer taking place along the short TBR, while keeping coarse axial meshes (20-30 cm) to limit the CPU time of a complete reactor sequence. In this sense, one of the most interesting approaches to overcome this issue was formulated was the one formulated by (Nelson and Unal, 1992). Following experimental observations of Ishii and co-workers, such model states that the heat transfer along the TBR follows a decreasing exponential function (over an empirical length), the maximum value being the Critical Heat Flux (CHF) at the quench front location. This model was implemented in the two-fluid and six-equation ICARE-CATHARE mechanistic severe accident code (developed at IRSN), which, in contrast to integral codes, is dedicated to the more detailed description of circuits thermal-hydraulics and in-vessel phenomena. With this tool, the model was validated using data from the PERICLES facility at CEA (France) and RBHT facility at PSU (USA) (Chikhi and Fichot, 2010). The model is also showed to be valid for partially degraded cores, as shown by the validation of ICARE-CATHARE on the QUENCH experiments at KIT (Germany) (Chikhi et al., 2012; Chikhi and Fleurot, 2012).

However, the transposition of this modelling approach to integral severe accident codes is not straightforward. Indeed, integral severe accident codes need to be fast running tools with the highest possible accuracy to support accident management studies. Therefore, they introduce simplifications in the number of equations, fluids and involved terms in the mass, momentum and energy balance equations in comparison to best-estimate system thermalhydraulics codes, which use a two-fluid model involving the resolution of two momentum equations. The integral ASTEC V2.1 severe accident code, developed at IRSN, uses by default a two-fluid and five-equation scheme to obtain the void fraction, pressure and temperature-velocity fields for the liquid and gas phases (Chatelard et al., 2016, 2014). However, a two-fluid and six-equation approach has been recently transposed from the IRSN in-house DRACCAR code (Glantz et al., 2018) as to give a more accurate prediction of the system thermal-hydraulics. This is in consonance with the MELCOR V2.2 integral severe accident code developed at SNL (Humphries et al., 2017), which also uses a two-fluid and six-equation scheme for the resolution of the system thermalhydraulics.

Currently, all reactor safety analyses conducted using ASTEC V2.1 are carried out with the five-equation scheme and considering that the heat transfer along the TBR is given by the droplet projection model (in the following referred as DROPLET model). This model sets a large, uniform and constant heat transfer coefficient above the quench front providing that there is enough water in the fluid mesh. However, it introduces important uncertainties in the calculations, since the value of such a coefficient quite depends on the local conditions in the vicinity of the front (Yadigaroglu et al., 1993). Therefore, IRSN has started to conduct analyses using the referred exponential heat flux model proposed by (Chikhi

and Fichot, 2010; Nelson and Unal, 1992), referred as EXPCHF model in this article (DRACCAR model in ASTEC V2.1 series).

In this context, the present article aims at presenting the improved reflooding validation results due to the new six equation description and determining the most appropriate modelling choice concerning the heat transfer along the TBR (DROPLET or EXPCHF) for the five and six-equation hydrodynamic models, keeping in mind that a five-equation description may still be requested for specific computationally expensive sequences. For such a task, code predictions have been validated using data from the PERICLES facility dealing with the reflooding of intact PWR cores (Digonnet and Veteau, 1989).

# 2 Description of selected physical models by ASTEC V2.1

## 2.1 The CESAR and ICARE modules

The ASTEC code (Accident Source Term Evaluation Code) aims at simulating the progression of entire severe accident sequences in nuclear water-cooled reactors, from occurrence of the initiating event up to the release of radioactive elements out of the containment. Its main field of applications are Severe Accident Management (SAM) and Level 2 Probabilistic Safety Assessment (PSA2) studies. The code is modular, each module describing a set of physical phenomena, which may take place during a severe accident. A detailed description of the scope of each ASTEC V2.1 module can be found in (Chatelard et al., 2016). Within this work, only the CESAR and ICARE modules are used.

The CESAR module describes the thermal-hydraulics throughout the primary and the secondary circuit, including the reactor pressure vessel. Within the core, the CESAR thermal-hydraulics modelling (Gómez-García-Toraño and Laborde, 2019) is based on a two-dimensional two-fluid and a five (by default) or six-equation approach (see 2.3 for hydrodynamics description of both models), including four differential conservation equations of mass and energy of gas and liquid. Both approaches are operative, but the latter still requires further validation, particularly for the analysis of core reflooding. On the other hand, the ICARE module handles the simulation of all in-vessel phenomena from the heat transfers in intact geometry to the core degradation and material relocation. In this study, the following heat transfers in intact geometry are concerned: conduction and gap heat transfers inside rods, and wall to fluid heat exchanges (convection, film boiling and radiative heat transfer to droplets and steam). Radiative heat exchanges between rods and the surrounding shroud are neglected: the temperature difference between the shroud and the rods is too low to generate a significant heat flux compared to the flux extracted by the fluid.

## 2.2 Modelling reflooding in ASTEC V2.1

The current reflooding model is only devoted to situations where water enters at the bottom of the core. In terms of quench front detection and heat transfer description, the model is valid regardless the core damage state and the selected hydrodynamic model. However, in terms of hydrodynamics, the momentum equation takes a different form depending on these, which in turn affects the calculation of the phase velocities and hence, the power extracted from the core. In the following, the article presents the main features of the reflooding model putting the special focus on intact geometries and the five and six-equation schemes. The modelling features presented hereafter are operational starting from the release of ASTEC V2.1.1.6.

### *2.2.1 Quench front detection*

For the calculation of the quench front position, ASTEC V2.1.1.6 follows a similar approach as the one followed in ICARE-CATHARE code (Chikhi and Fichot, 2010). The code postulates that the wall temperature profile upstream the quench front is flat due to the strong cooling of the wall by the quench front, down to a temperature close to the saturation temperature (the value $T_{sat}$+5 was selected). Besides, it considers that the temperature profile downstream the quench front is flat with values higher than minimum film boiling temperature $T_{MFB}$. Finally, the temperature profile along the TBR is approximated by a step, where the lower bound is the temperature of the first mesh below the quench front (index *IQF-1*) and the upper bound is the temperature of the first mesh above the quench front (index *IQF+1*). The quench front mesh (*IQF*) is defined as the first mesh (starting from the bottom of the wall) where the wall temperature is higher than $T_{sat+5}$, providing that the temperature of the mesh *IQF+1* is higher than $T_{MFB}$ and the void fraction in the mesh *IQF* is lower than 0.9999. The elevation ZQF of the quench front in this mesh is computed as a function of the current temperature in the mesh *IQF*, ensuring a regular progression of the quench front in the mesh.

### *2.2.2 Heat transfer along the TBR*

As already pointed out in the introduction, ASTEC has two different models to describe the heat transfer along the TBR, these being the DROPLET and the EXPCHF models (the latter formerly known as DRACCAR model).

The DROPLET model postulates the existence of a large heat transfer coefficient $H_D$ (by default 150 W/m$^2$/K) towards the interface in all meshes over a distance $Z_D$ (by default 0.8 m) above the quench front elevation ZQF. This heat transfer is applied to evaporate the water in a given mesh, providing that its void fraction is lower than $\alpha_D$ (by default 0.999), the heat transfer being given by Eq. 1. Therein, $T_{liq}$ is the temperature of the liquid in the current mesh and $T_{wall}$ is the temperature of the wall in contact with the liquid. The variables $H_D$, $Z_D$ and $\alpha_D$ are user-dependent and have a considerable impact on model predictions. The default values were obtained following an internal study involving a sensitivity analysis on several PERICLES experiments with the CESAR five-equation scheme. The default values of the

DROPLET model are the ones minimizing the relative error between the computed and the experimental evolution of the quench front progression and cladding temperature at selected elevations.

$$\varphi_{TBR}^{DROPLET}(z) = H_D \times \left(T_{wall} - T_{liq}\right) \quad \text{Eq. 1}$$

As for the EXPCHF model, the heat flux is described by a decreasing exponential function (see Eq. 2), following the formulation proposed by (Nelson and Unal, 1992) and later on adopted by (Chikhi and Fichot, 2010). Therein, *CHF* represents the critical heat flux, z the absolute elevation of the section where the heat transfer is evaluated and $L_1$ the characteristic length over which this heat transfer is applied. Alike (Glantz et al., 2018), the *CHF* is calculated using Zuber's correlation for pool boiling with the correction on liquid subcooling due to Ivey and Morris (Ivey and Morris, 1962). This is in contrast to (Chikhi and Fichot, 2010), who calculated the *CHF* using the Groenenveld look-up table and additionally included a dependency with the liquid velocity and the void fraction near the quench front. The later approach could be implemented in the future.

$$\varphi_{TBR}^{EXP-CHF}(z) = CHF \times e^{\frac{ZQF-z}{L_1}} \quad \text{Eq. 2}$$

Such modelling takes advantage of previous experiments performed by Ishii and co-workers (Obot and Ishii, 1988), who observed that the $L_1$ associated to each flow regime (smooth, rough wavy, agitated, dispersed) depended on the capillary number according to Eq. 3. The liquid velocity is calculated at the junction between the meshes *IQF* and *IQF-1*. However, such observations did not identify an expression of $L_1$ for the TBR, which egged on (Nelson and Unal, 1992) and then (Chikhi and Fichot, 2010) to propose correlations based on the capillary number with the form given by Eq. 4. In both studies, the constant $C_1$ took two different values depending whether *Re*>2000, the value in each regime being different in both studies (an order of magnitude higher in (Chikhi and Fichot, 2010)). Due to the similarity between ASTEC and ICARE-CATHARE, this work adopts the values described in (Chikhi and Fichot, 2010). Expression given by (Nelson and Unal, 1992), with a $C_1$ coefficient an order of magnitude lower, have also been tested in ASTEC but the length of the TBR zone was then very short and the reflooding (if any) was too slow in all PERICLES tests. This can be explained by two remarks. First, the values applied in (Nelson and Unal, 1992) are deduced from steady-state experiments in which the TBR may be shorter than in reflooding conditions. Second, the model of (Nelson and Unal, 1992) accurately describes all regimes downstream the quench front (TBR but also inverted annular flow and dispersed flow in which the heat transfer can also be efficient) while only one specific regime is described in ASTEC, covering a larger region.

$$Ca = \frac{\mu_L v_L}{\sigma_L} \quad \text{Eq. 3}$$

$$L_1 = C_1\, Ca^{0.5} \qquad \text{Eq. 4}$$

At this point, it is worth mentioning that the liquid velocity used to calculate the capillary number contains a correction factor depending on the selected hydrodynamic model. This is done to keep $L_l$ within the physically sounded value of few centimetres. This way, $(1-\alpha)v_L$ is used in the five-equation scheme to correct the high liquid velocities associated with high void fractions i.e. residual presence of the liquid phase. Conversely, $v_L$ is used in the six-equation scheme without correction since the latter can deal with the presence of residual phases. Therefore, the introduction of such a correction factor allows calculating a length $L_l$ that stays within physical bounds (few centimetres) regardless of the selected hydrodynamic model.

A sketch of the heat flux profiles associated to the EXPCHF and DROPLET models is depicted in Figure 1. Therein, the real flow patterns corresponding to a situation of a low-quality CHF (e.g. high flow rates, high pressures) and a high-quality CHF (e.g. low flow rates, high electrical powers) have been also included. The solid red line is the calculated one during the simulation whereas the dashed one is the hypothetical one (if the restrictions of $\alpha_D$ and $L_l$ did not apply). As it is observed, the TBR length calculated by the two models is not necessarily the same. Indeed, in the DROPLET model this length is limited by $Z_D$ or, more likely, by the unavailability of water in the mesh $\alpha_D$, whereas in the EXPCHF the length is limited by the characteristic length $L_l$. In the EXPCHF model, $\alpha_D$ can also be limiting.

Currently, all reactor safety studies performed use CESAR in five-equation mode and reflooding calculations are launched using the DROPLET model. Nevertheless, IRSN is pursuing an intense validation effort to possibly replace the DROPLET model by the EXPCHF model which is more physical-sounded and less user-dependent.

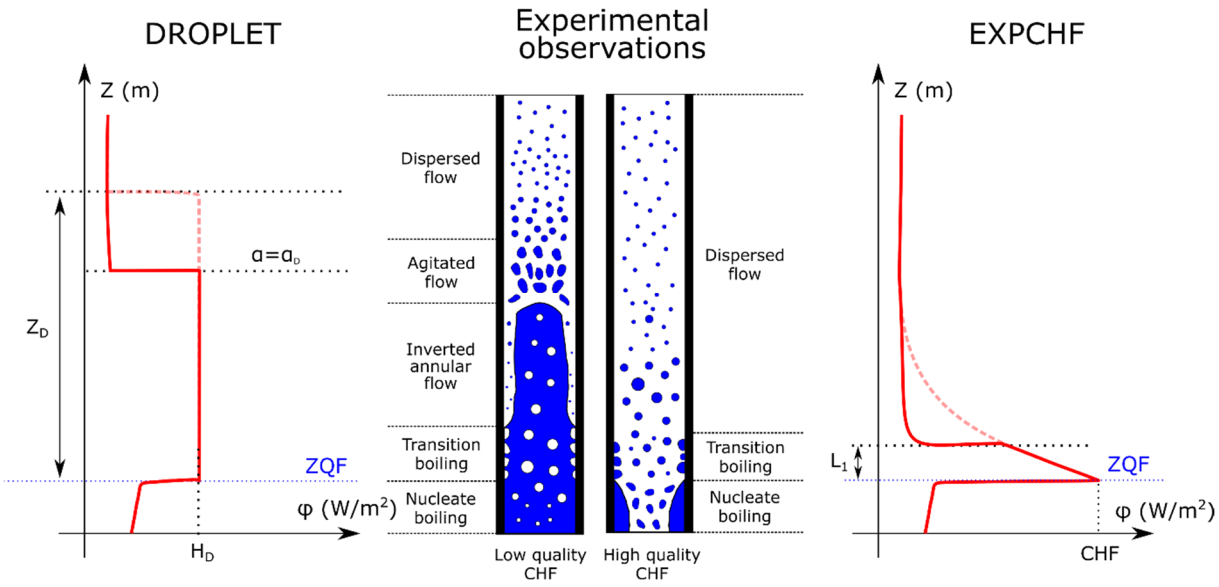


Figure 1: Sketch of axial parietal heat fluxes calculated along the TBR by the (left) DROPLET and (right) EXPCHF models. Experimental observations for low and high-quality CHF can be found at the centre and are based on (Nelson and Unal, 1992).

### *2.2.3 Heat transfer correlations in other flow regimes*

As far as the rest of boiling heat transfer mechanisms are concerned, nucleate boiling below the quench front is evaluated with the Thom correlation (Thom et al., 1965), whereas film boiling above the TBR is evaluated with the Berenson correlation (Berenson, 1961).

## 2.3 Hydrodynamic aspects

The summary of the different terms considered in the momentum conservation equation for the five and six-equation hydrodynamic models without the presence of porous media were already introduced in (Gómez-García-Toraño and Laborde, 2019). For the sake of understanding, this section gives a short reminder on both numerical schemes implemented in CESAR.

For the five-equation scheme, one momentum balance equation on the mean phase velocity is solved for all junctions. Assuming that the flow along the test section is one-dimensional and that the cross section is uniform, the average momentum balance equation for the junction *J* along the flow direction can be written according to Eq. 5. Therein, the first term represents the axial pressure gradient, $F_M^{reg}$ and $F_M^{sing}$ the regular and singular friction terms, $F_M^{adv}$ the advection term, $F_M^{grav}$ the hydrostatic pressure gradient and $I_M$ the inertial term computed with the averaged fluid velocity.

$$\frac{\partial P}{\partial z} + F_M^{reg} + F_M^{sing} + F_M^{adv} + F_M^{grav} + I_M = 0 \qquad \text{Eq. 5}$$

Additionally, the five-equation scheme introduces an algebraic equation for the calculation of the drift velocity between the gas and liquid phases ($\Delta V$). For vertical junction, the drift velocity can be written

according to Eq. 6. Therein, $F(\bar{\alpha})$ is a smoothing function depending on the mean void fraction, whereas $F_{NR}$ is the non-stratification friction term which depends on the geometry, flow configuration and other thermodynamic parameters (Wallis, 1969). Such expression is evaluated if the presence of both phases is not residual ($0.05 < \alpha < 0.95$), and it is set to zero (equity of gas and liquid velocities) in the rest of cases.

$$\Delta V = V_G - V_L = F(\bar{\alpha}) \sqrt{\frac{g(\rho_L - \rho_G)}{F_{NR}}} \qquad \text{Eq. 6}$$

The five-equation scheme is suitable for quasi-steady developed flows in pipes without strong phase changes and with $0 < \alpha < 0.7$. However, for accelerating flows (where the advective term is significant), a six-equation scheme involving two sets of momentum conservation equations in each phase have better capabilities (Bestion, 2011). Considering a one-dimensional flow, a uniform test section and neglecting the capillary forces (pressure of the liquid and the gas are similar and equal to P), the two momentum balance equations for the liquid and gas phases projected along the flow direction at the junction *J* can be written as follows:

$$\bar{\alpha}_L \frac{\partial P}{\partial z} + F_L^{reg} + F_L^{sing} + F_L^{adv} + F_L^{grav} - F_{LG}^{int} + I_L = 0 \qquad \text{Eq. 7}$$

$$\bar{\alpha}_G \frac{\partial P}{\partial z} + F_G^{reg} + F_G^{sing} + F_G^{adv} + F_G^{grav} + F_{LG}^{int} + I_G = 0 \qquad \text{Eq. 8}$$

It is observed that the interfacial friction between the liquid and gas phases $F_{LG}^{int}$ is now explicitly considered. For a vertical non-stratified flow, the expression is given by Eq. 9. Therein, $f_{int}(\alpha)$ represents the interfacial friction coefficient, integrating the effects of geometry and flow configuration. It can be obtained using a number of correlations, as explained in (Wallis, 1969).

$$F_{LG}^{int} = f_{int}(\alpha) \cdot \bar{\alpha}_L \cdot \bar{\alpha}_G \cdot \Delta V \cdot |\Delta V| \qquad \text{Eq. 9}$$

In terms of numerical stability, the two schemes have similar behaviour while the five-equation scheme converges slightly faster in general. Numerical issues are more related to the reflooding models than to the hydrodynamic model: in the DROPLET model, the quench front progression from mesh to mesh is associated with large heat flux peaks because of different fluid conditions from one mesh to another. This issue is less pronounced in the EXPCHF model in which the accurate quench front location is used to distribute heat fluxes on a continuous way upstream and downstream the quench front.

# 3 The PERICLES Experimental facility

## 3.1 Experimental setup

The PERICLES experimental program at CEA Grenoble (France) mainly aimed at improving the understanding on core thermal-hydraulics during the reflooding phase of a PWR (Digonnet and Veteau, 1989; Housiadas et al., 1989). The test section consists of an insulated stainless-steel shroud, which entails 368 electrically heated fuel rod simulators (FRSs) and 25 stainless steel guide tubes in a 17x17 geometry. Each FRS is electrically heated over 3656 mm and consists of three helical nichrome V wires, which are embedded into a boron nitride matrix. Stainless steel claddings surround the FRSs. The wire density is varied along the FRSs in order to obtain a PWR-representative cosine shape power distribution around the centre with an axial peaking factor of 1.6. A sketch of the test section is shown in Figure 2.

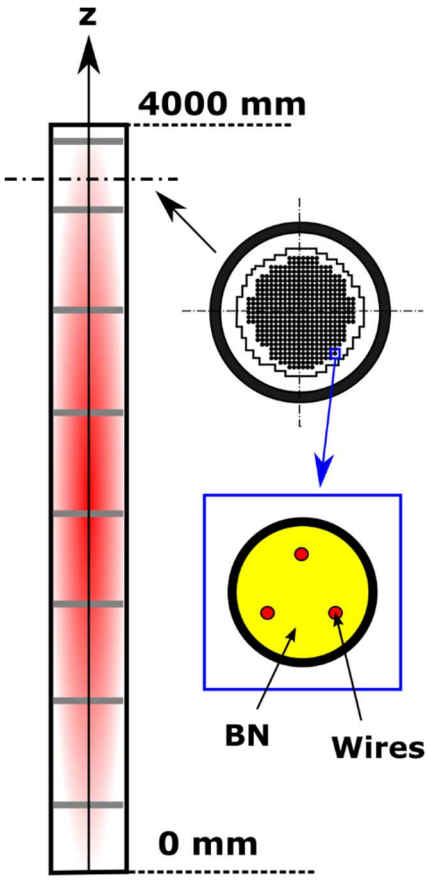


Figure 2: Sketch of the PERICLES test facility.

In all reflooding tests, the electrical power is supplied to the FRSs, the injection being launched when maximum temperatures reach a set point and stopped when the core is refilled. Influence of pressure, heating power, injection mass flow rate and initial temperature were studied. Several tests with a wide range of pressures, mass flow rates, electrical powers and initial temperatures have been used to validate the code. The list of tests can be found in Table 1. The initial temperature at the hottest part of the bundle is 600°C for all tests. Mass flow rates are ranging between 1-5 g/cm$^2$/s, which corresponds to nominal

injection velocities of 10-50 mm/s (35-180 m/h). It is worth pointing out that the High- and Low-Pressure Injection Systems (HPIS, LPIS) of a French PWR 900 $MW_e$ generally consist of three trains, each of them giving nominal flow rates of 50 kg/s (HPIS) and 100 kg/s (LPIS). These correspond to injection velocities of about 9-18 mm/s (equivalent to 30-60 m/h), which are equivalent to those used in PERICLES experiments.

The assembly temperature field is mapped through thermocouples (THCs) located at different elevations along some FRSs. Pressure along the longitudinal axis can be measured through differential pressure transducers. The liquid mass flow rate injected and the steam mass flow rate exiting the bundle can be measured by two different flow meters. The quench front is assumed to reach a given axial location when the temperature of the nearest thermocouple falls below $T_{sat}$+5. No significant uncertainties can be attributed to the measurements, as pointed out in (Digonnet et al., 1988).

Table 1: Selected Pericles experiments for the validation of the ASTEC V2.1 reflooding model. All tests have an initial temperature of 600 ºC, which is larger than $T_{MFB}$ (condition required to apply the reflooding model). Tests with non-constant electrical power have been excluded from this study.

| Name | Pressure (bar) | Electrical power ($W/cm^2$) | Flow rate ($g/cm^2$ s) | Subcooling (ºC) |
|---|---|---|---|---|
| p1 | 3 | 3.35 | 3.6 | 60 |
| p5 | 3 | 3.35 | 2.5 | 60 |
| p7 | 3 | 3.35 | 5 | 60 |
| p8 | 3 | 3.35 | 8 | 60 |
| p9 | 2 | 3.35 | 3.6 | 60 |
| p11 | 4 | 3.35 | 3.6 | 60 |
| p12 | 3 | 3.35 | 3.6 | 60 |
| p13 | 3 | 3.35 | 13 | 60 |
| p25 | 3 | 4.20 | 5 | 60 |
| p27 | 3 | 4.20 | 3.6 | 60 |
| p712 | 20 | 2 | 1.7 | 4 |
| p74 | 20 | 2 | 3 | 4 |
| p75 | 20 | 2 | 3 | 4 |
| p77 | 40 | 2 | 3 | 7 |
| p80 | 10 | 1 | 3 | 1 |

### 3.2 Modelling in ASTECV2.1

The ASTEC V2.1 model of the experimental bundle consists of one weighted rod, representing the 368 electrically heated FRSs, and one weighted hollow tube, representing the 25 guide tubes. Each FRS consists of a stainless-steel cladding and a fuel pellet, which encloses an inner and outer cylinder of boron nitride and a heated nichrome cylinder in between. The density of the nichrome cylinder varies along the active bundle length in order to reproduce the experimental power deposition. Both the FRSs and the guide tubes are surrounded by a shroud.

The bundle is axially discretized in 18 meshes giving an axial mesh height of about 200 mm, which corresponds to the current recommendation for reactor calculations with ASTEC. The axial discretization was the result of an iterative procedure: the study originally considered 30 axial meshes. Then, axial refinement was progressively decreased down to an optimal value below which the prediction on the key figures of merit (quenching time and peak cladding temperature) started to be impaired. Concerning radial discretization, only one radial mesh has been considered when modelling the PERICLES test section. This radial discretization is justified because the tests were generally characterised by a one-dimensional quench front progression. However, some tests involving high mass flow rates and/or high heating powers and low pressures (e.g., p7) showed top flooding at the upper part of the bundle, which implies the existence of multi-dimensional effects. A finer radial discretization will be used in future validation studies on the 2-D PERICLES, where two-dimensional effects were more visible.

The temperature, pressure and mass flow rate vary according to the experimental values along the calculation. A pressure boundary condition is set at the bundle outlet, the values being varied according to the experimental data along the calculation.

## 4 Results using CESAR five-equations

### 4.1 Results using the DROPLET reflooding model

A set of predictions using the current reflooding model in CESAR five-equations is carried out for tests named p5 and p7, which differ only by the reflooding mass flow rate (see Table 1) and compared with experimental results. The quench front progression and the cladding temperature evolution at z=2550 mm (i.e. hottest bundle region) are shown in Figure 3.

The experimental temperature evolution hints the existence of four differentiated phases regardless the mass flow rate: heat-up phase, precooling, quenching and saturation. It is observed that the heat-up and pre-cooling phases are longer as the injected mass flow rate decreases. Indeed, a decrease of the mass flow rate reduces the quench front velocity and enhances the dispersion of the flow above the front, the last factor contributing to a shortening of the TBR.

As far as code predictions are concerned, CESAR five-equations provides a good representation of the experimental data when mass flow rates are higher than 3.6 g/cm$^2$ s e.g. p7 and p12 tests. However, the quenching times become increasingly underestimated as the mass flow rate decreases below that value, as shown in the prediction of the test p5. The behaviour is congruent with the earlier quenching of the cladding. The behaviour of the cladding temperature at z=2500 mm during the first instants of the transient is of special interest. Within that time window, the quench front remains below z=1700 mm, this meaning that the DROPLET model (which is applied over a distance $Z_D$ = 800 mm) should not have a strong impact on the cladding temperature. Nevertheless, cladding temperatures are underestimated during that time gap of the heat-up and the precooling phases. This shows that the code overestimates the water availability far above the quench front for low reflooding mass flow rates. This point will be further discussed in section 5 when comparing the five and six-equation schemes.

It is noticed that ASTEC results predict bottom flooding at all bundle elevations whatever the mass flow rate. This is in contrast to the experimental results, where bottom and top flooding may take place, especially for high mass flow rates (p7). Indeed, a higher mass flow rate enhances 2-D effects in the bundle, leading to a faster progression of the water near the wall. Eventually, part of this water falls down back to the upper core regions. This top flooding mechanism, which is relevant as the mass flow rate increases, cannot be captured by the geometrical ASTEC model. This could be already anticipated, since only one radial mesh has been used to describe the core fluid region in the current ASTEC model (section 3.2). The modelling of top flooding is out of scope for this article, but future improvements in this area are foreseen.

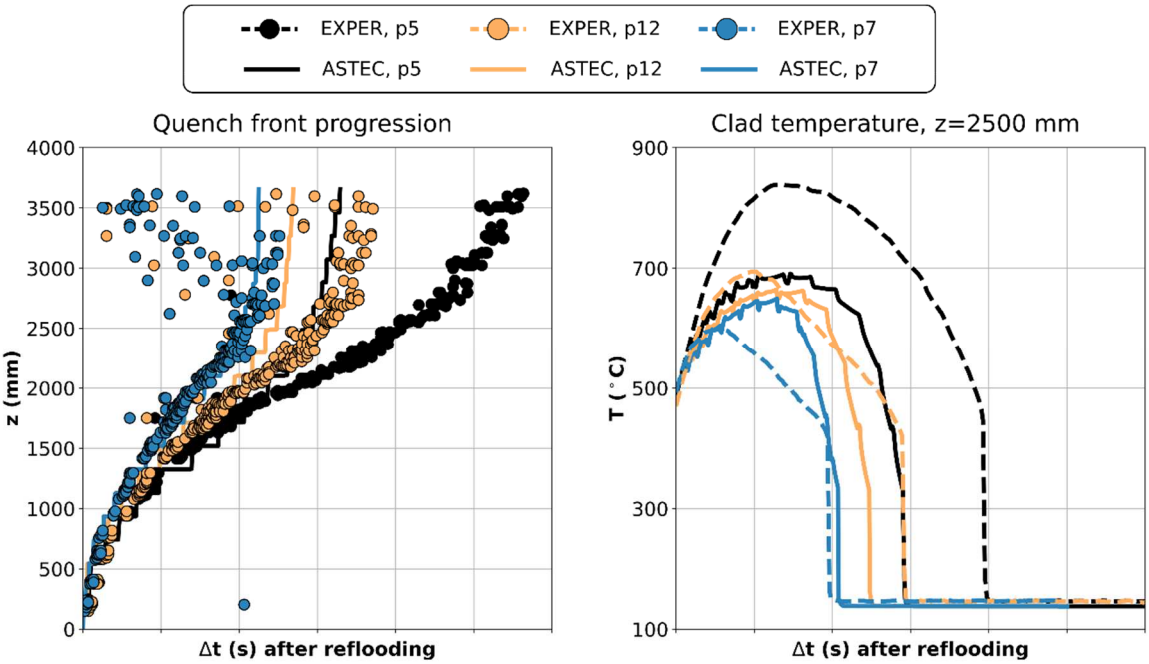


Figure 3: Comparison of the predicted and experimental temporal evolutions of the quench front location and the cladding temperature at z=2500 mm. Predictions correspond to the DROPLET reflooding model using CESAR five-equations on tests with different flow rate.

### 4.2 Comparison of DROPLET vs. EXPCHF reflooding models

The previous section has shown that the DROPLET model predicts faster refilling times than the experimental ones as the injected flow rate decreases because of the stronger precooling associated with the choice of the reflooding model and the hydrodynamic model. Despite this deviation has a lot to do with the 5-equation model, it is still interesting to study the individual influence of the DROPLET and EXPCHF models. The comparison of the experimental and computational temporal evolution of the quench front and cladding temperature, steam generation rate and water flow rate at z=1800 mm is depicted in Figure 4 for the test p5. That elevation is taken to better illustrate the differences between the two reflooding models.

The choice of the model significantly affects the quench front progression and the cladding temperature evolution. Indeed, the DROPLET model manages to evacuate the heat stored in the fuel rod, which is the reason why the quench front reaches the top of the bundle. In contrast, the EXPCHF model cannot evacuate enough heat in the vicinity of the quench front, this leading to temperature escalation and increasing difficulty for quench front progression. The figure also shows that code predictions slightly underestimate the cladding temperature during the first instants of the transient, this becoming more apparent for higher cladding elevations.

The contrast of the behaviour can be explained in terms of the length over which each model is applied. To explain this, the attention is focused on the instant $t^A$. At that time, the quench front is located at z=1200 mm for both simulations, but the behaviour at z=1800 mm is considerably different. Indeed, the

DROPLET model leads to an important evaporation, which increases when the quench front approaches that section. This happens because the mesh located at z=1800 mm has enough water and because it lies within the $Z_D$ length imposed by the DROPLET model. Hence, the $H_D$ heat transfer coefficient is applied. Conversely, EXPCHF calculates a weaker evaporation, since a film boiling regime is detected by the code. This is consistent with the higher liquid flow rates at z=1800 mm.

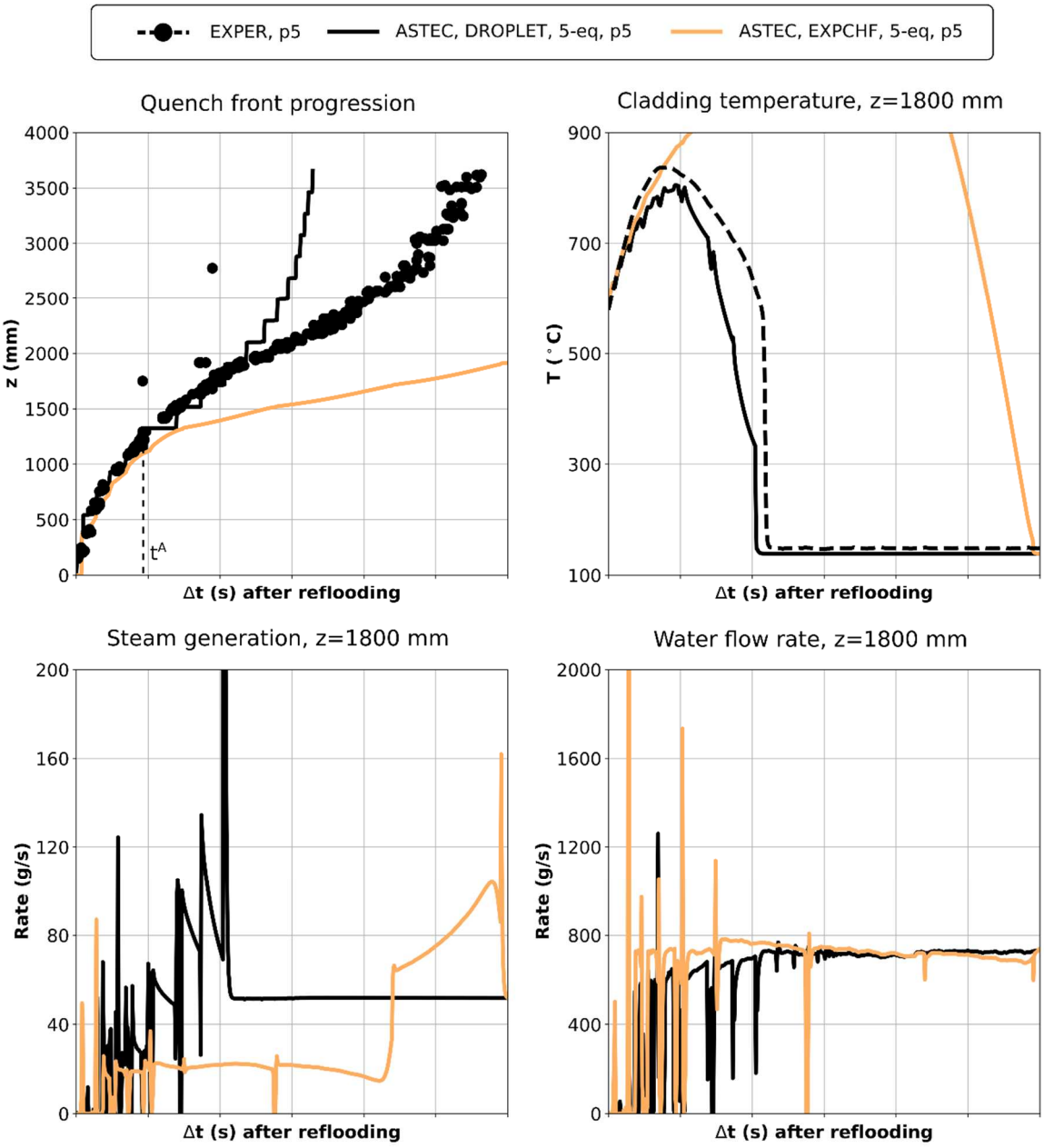


Figure 4: Influence of DROPLET and EXPCHF heat transfer models on the temporal evolution of the quench front progression and the cladding temperature, steam generation rate and water flow rate at z=2500 mm for the test p5. Predictions obtained using CESAR five-equations.

# 5 Comparison CESAR five vs. six equations

The previous section has shown that the five-equation scheme only provides reasonable results when the DROPLET reflooding model is used. The aim of this section is to determine if the six-equation scheme and the DROPLET or EXPCHF reflooding models provide a better representation of the experimental results. To discuss this appropriateness, the experimental and predicted quench front progression, cladding temperature at z=2500 mm and integral steam mass at the outlet are represented in Figure 5 for the test p5. Black scattered dots and dashed lines represent the experimental data; solid lines are associated to predictions with the five-equation scheme, whereas dotted lines with the six-equation scheme; the blue colour is associated with the DROPLET model whereas the orange one with EXPCHF.

It is observed that the EXPCHF reflooding model together with the six-equation scheme provides a good agreement with the experimental results, unlike the same model being used with the five-equation scheme. In particular, the quench front can now rise to the top of the bundle because of the stronger precooling predicted by the six-equation scheme near the quench front, which is reflected in the cladding temperature evolution. For identical reasons, predictions using the DROPLET model and the six-equation scheme are worse than those obtained when using the five-equation scheme. Moreover, for a given numerical scheme, DROPLET predicts a faster refilling than EXPCHF because of the longer extension over which this model is calculated together with its high heat transfer coefficient $H_D$.

Cladding temperatures at z=2500 mm are underestimated at the beginning of the transient for either scheme or reflooding model, even if the quench front is well below that location. This indicates that, for the test p5 involving a low mass flow rate, either scheme predicts a greater water availability well above the quench front in comparison to the experiment. The modelling of the small-droplet disperse flow regime will require further improvements for either numerical scheme. In turn, this stronger precooling leads to an acceleration of the quench front at the second half of the bundle for almost all cases.

An analysis of the integrated steam mass along the experiments shows that almost three out of four simulations can predict the experimental steam mass at the end of the experiment. For these scenarios, the bundle can be cooled down, the initial energy being extracted by water injection. It is noticed that the use of the EXPCHF model together with CESAR five-equations is significantly lower than the experiment and the rest of simulations, which indicates difficulties in terms of core cooling. The reader can observe that the slopes in the curves of the steam mass relate to the quench front velocity. In particular, the use of the DROPLET model grows quickly at the beginning of the transient, then becomes increasingly deviated from the experimental because of the underestimation of PCTs.

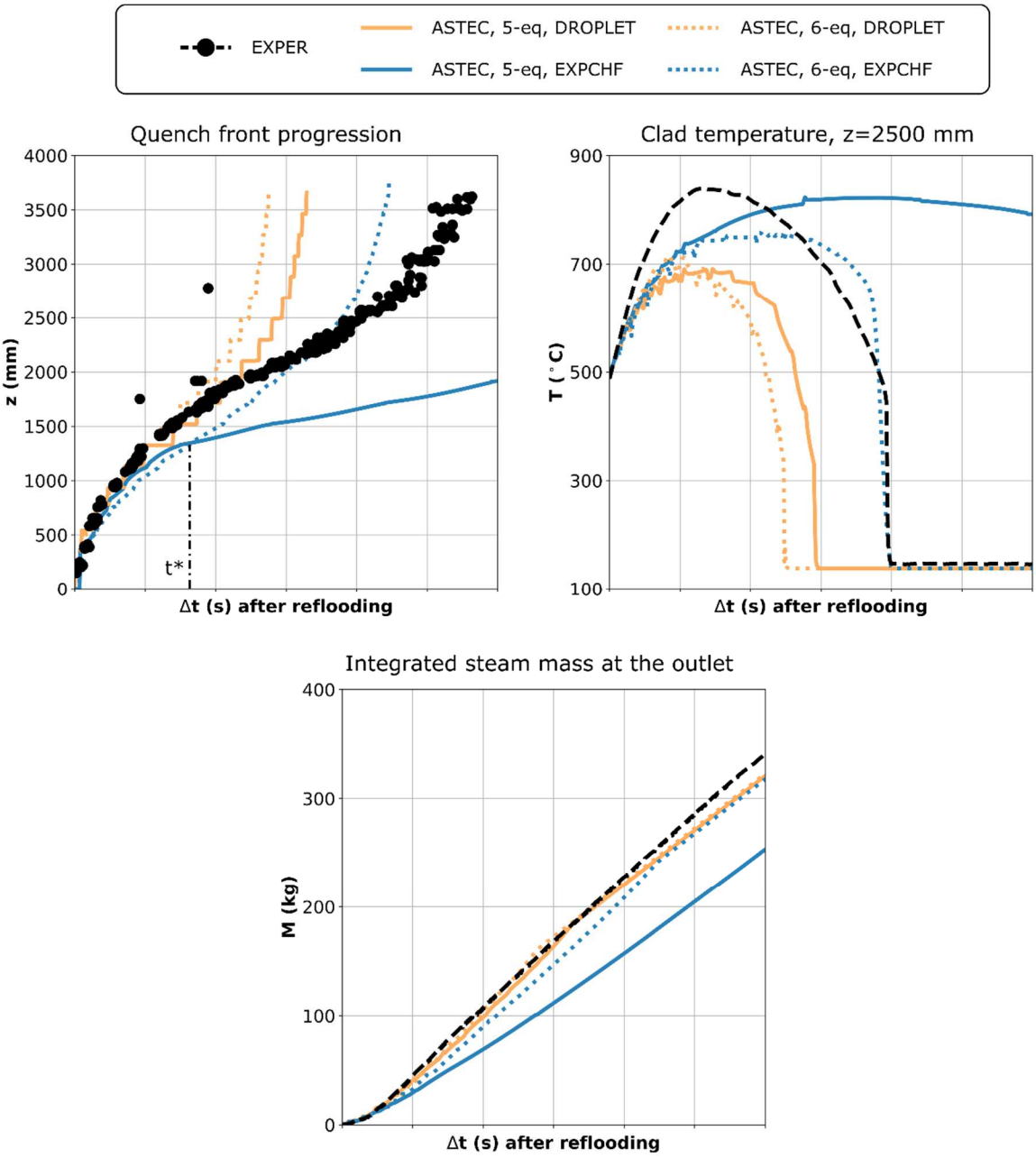


Figure 5: Comparison of the predicted and experimental evolution of the quench front progression, cladding temperature at z=2500 mm, total steam mass at the outlet for the test p5.

To better understand the differences between the five and six-equation schemes, selected axial profiles corresponding to predictions with the EXPCHF reflooding model are depicted in Figure 6 for the test p5 at t=t*. This instant is chosen because it is the last one before the quench front progression starts to differ in both simulations. Indeed, the quench front elevation is represented by a horizontal dashed blue line in all subplots of the figure, which indicates that its location is the same at t* for both simulations.

On one hand, the five-equation scheme leads to the prediction of significant liquid velocities above the quench front, since the drift velocity is set to zero for void fractions higher than 0.95 (see section 2.3). Hence, the available liquid is instantly made available in all meshes above the quench front. Part of this

water is transformed into steam (especially along the TBR), but nearly 40 % of the mass flow rate exits the bundle without contributing to the overall cooldown, as shown in axial water flow rate. On the other hand, the six-equation scheme leads to differentiated phase velocities regardless the void fraction because two equations on phase velocities are solved. The prediction of small liquid velocities, which is congruent with the lower void fraction, ensures that the liquid mass is kept near the quench front. Therefore, the steam generation rate along the TBR is generally more intense in the six-equation scheme than that predicted by the five-equation one.

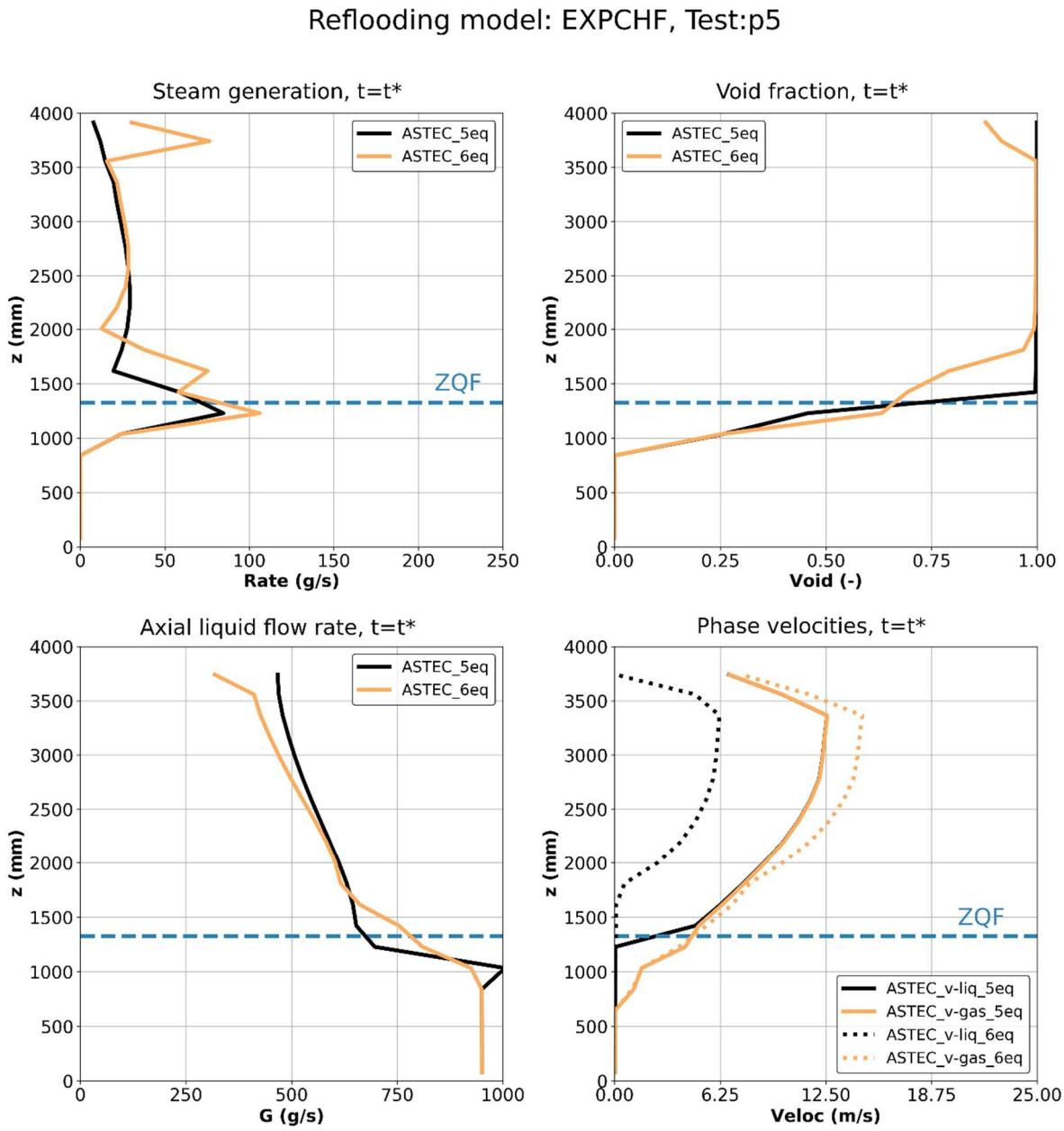


Figure 6: Comparison of CESAR five vs. six equations using the EXPCHF reflooding model on selected axial profiles at time=t* for the test p5. The quench front elevation at t* is represented by a single horizontal blue line for both simulations.

Calculations on further PERICLES reflooding experiments have been launched using a combination of the presented hydrodynamic model and heat transfer reflooding models. For each calculation, the time needed by the quench front to reach 2500 mm and the Peak Cladding Temperature is retrieved. Results can be found in Figure 7 and Figure 8. The elevation of 2500 mm is convenient because of the inexistence of top flooding for all experiments, in contrast to higher elevations. The thermal-hydraulic features of each experiment can be found in Table 1.

At first glance, neither the hydrodynamic model nor the reflooding model affect the quenching time at high pressures (p74, p75, p77, p80) or high mass flow rates (p8 and p13), predictions being close to the experimental data. Indeed, experiments involving high pressures are characterized by a relatively long inverted annular flow region above the quench front, followed by an agitated region of slugs and by a small-droplet dispersed flow region (Ishii and De Jarlais, 1987; Obot and Ishii, 1988), which in turn lead to a strong heat removal from the wall. Therefore, an agreement between experimental data and code predictions exists because a significant precooling is predicted whatever the combination of the reflooding model or the hydrodynamic model. However, the agreement on the quenching time is not completely reflected in the Peak Cladding Temperature. This is related to the overestimation of the heat transfer in the dispersed flow region, as already shown in Figure 5. Future improvements on the description of the small-droplet dispersed flow region are foreseen.

The rest of tests are characterized by combinations of electrical power, system pressure and mass flow rates in such a way that the flow ends up being highly dispersed. In those cases, a precise estimation of the precooling is necessary for a correct prediction of the quench front progression. It is observed that DROPLET predicts a faster refilling than EXPCHF regardless of the hydrodynamic model because of the higher integrated heat flux along the TBR, which spans over a considerable distance $Z_D$. As far as the hydrodynamic model is concerned, the six-equation scheme predicts a faster refilling than the five-equation scheme because of the higher availability of water near the quench front, as shown previously in this chapter. For those tests, the agreement with the PCT is satisfactory. This is especially true for the six-equation scheme together with the EXPCHF model, which predicts a slighter precooling than calculations the DROPLET model with either numerical scheme. Yet, predicted precooling is stronger than the experimental one, as reflected in the slight underestimation of the PCTs. Finally, it is observed that the EXPCHF together with five equations clearly overestimates PCTs, which is a direct consequence of the longer quenching times.

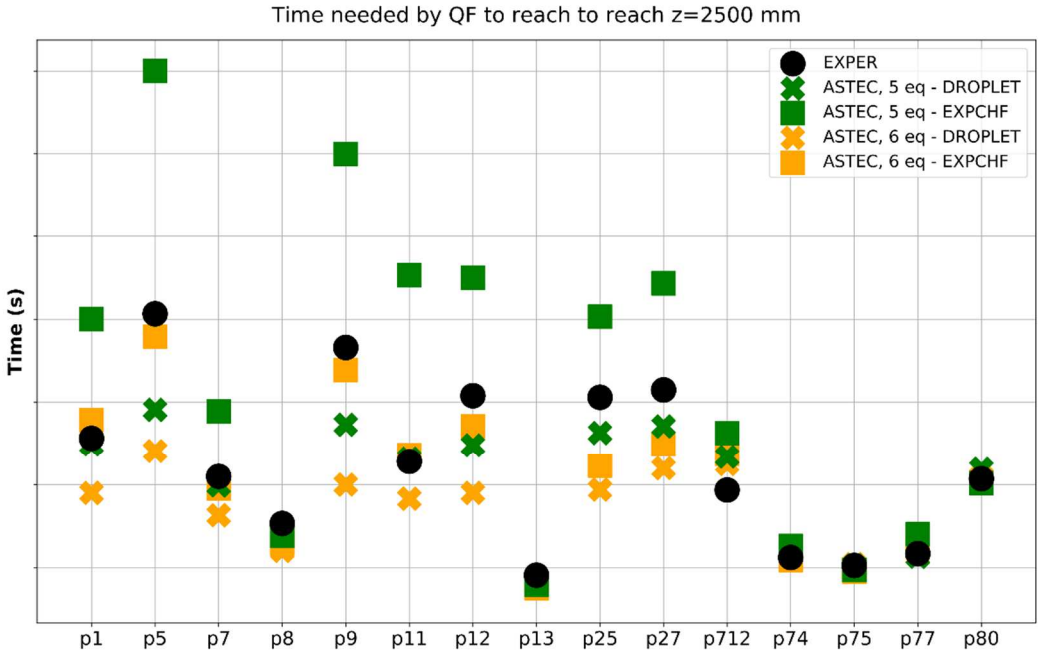


Figure 7: Predicted times to quench the fuel rods up to 2500 mm using the DROPLET or EXPCHF reflooding models together with CESAR five or six-equations vs. experimental data.

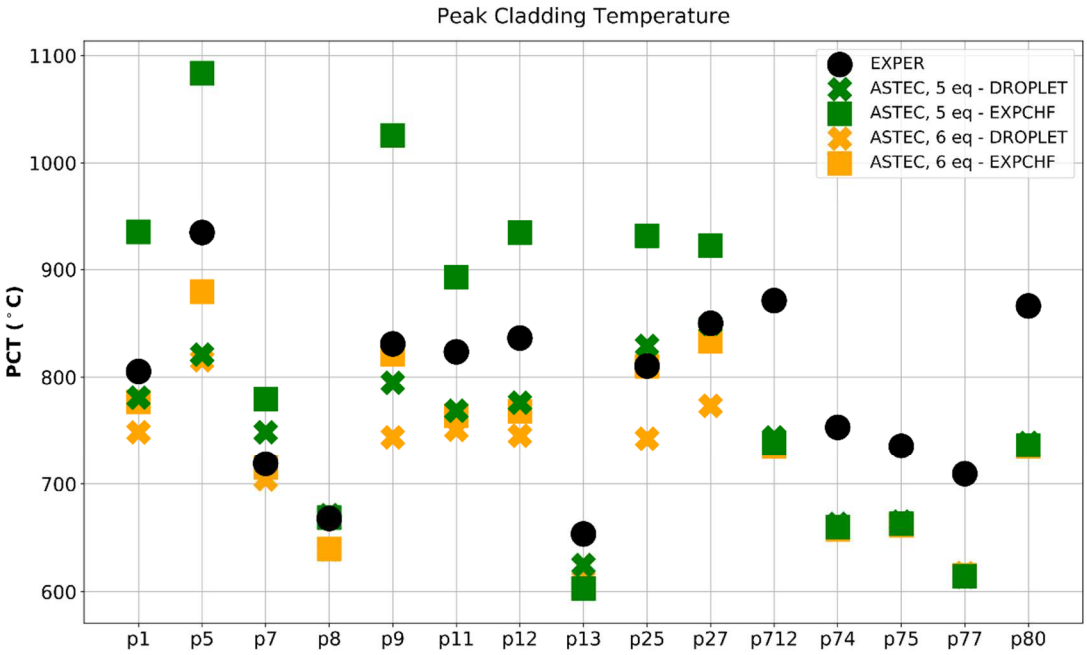


Figure 8: Predicted Peak Cladding Temperature along the transient using the DROPLET or EXPCHF reflooding models together with CESAR five or six-equations vs. experimental data.

# 6 Discussion

To support the decision on the most suitable model for either scheme, the relative error of the fuel rod quenching time at z=2500 mm (with respect to the experimental data) for each PERICLES test has been depicted in Figure 9. The red bands represent the relative error of ±20%, which is the maximum deviation admissible for severe accident codes. This variable has been selected because of its importance for accident management. Indeed, it is essential to know whether a given injection can cool down the core and the time needed for such aim. Relative error on PCT is not shown, since all calculations lie within the limits of ±20% regardless of the combination of heat transfer model and hydrodynamic scheme.

Results show that the most suitable modelling of the heat transfer along the TBR depends on the choice of the hydrodynamic scheme. In particular, if the five-equation scheme is used, the best choice is to only rely on the DROPLET model with reasonable values of heat transfer coefficient and TBR length. However, if the six-equation scheme is used, the EXPCHF model alone can cool down the wall in the quench front vicinity. Even if predictions generally lie within the admissible error band, none of the two combinations provide a perfect match for all experiments. For example, five-equations plus DROPLET have difficulties to predict p5 and p9 tests, characterized by a high electrical power, whereas six-equations plus EXPCHF have difficulties to predict p25 and p27 tests, characterized by a combination of low mass flow rates and pressures. This is related to the difficulties experienced by integral severe accident codes to provide an accurate description of precooling when the dispersed film boiling is dominant, as it is the case for the considered thermal-hydraulic conditions.

The computational costs of both modelling options are shown in Figure 10. It can be generally stated that the use of six-equations plus the EXPCHF model does not significantly impair computational costs with respect to the five-equation scheme plus the DROPLET model. In fact, it sometimes requires a lower computational cost even if both modelling options predict an identical refilling time (see p7, p8 and p25 tests simulations in Figure 7). Hence, the computational cost should not be in this case the decisive factor to choose the most adequate modelling option. However, reactor calculations should be carried out to verify this point.

The two options seem appropriate to represent the core reflooding, but the EXPCHF model together with six-equation scheme brings more physical meaning to the system. The model also allows a reduction of the user effect and hence contributes to narrow uncertainty margins, since all its main parameters have been derived from experimental observations (Ishii and De Jarlais, 1987; Obot and Ishii, 1988). It is reminded that the DROPLET model considers fixed coefficients to describe the length and heat transfer associated with the TBR. This is in contradiction to existing experimental studies, which suggest that the magnitude of precooling depends on the local thermal-hydraulic conditions near the front (Yadigaroglu et al., 1993).

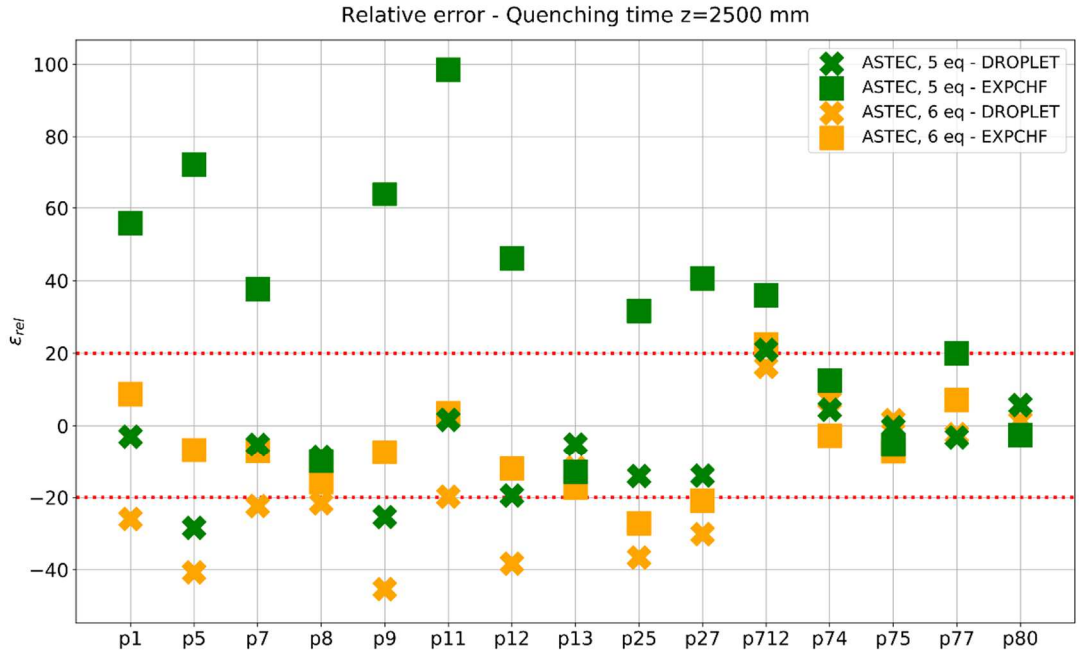


Figure 9: Relative error in the prediction of the quenching time of the fuel rods up to 2500 mm. Dotted red lines indicate a relative error of $\pm 20\%$ with the experimental data.

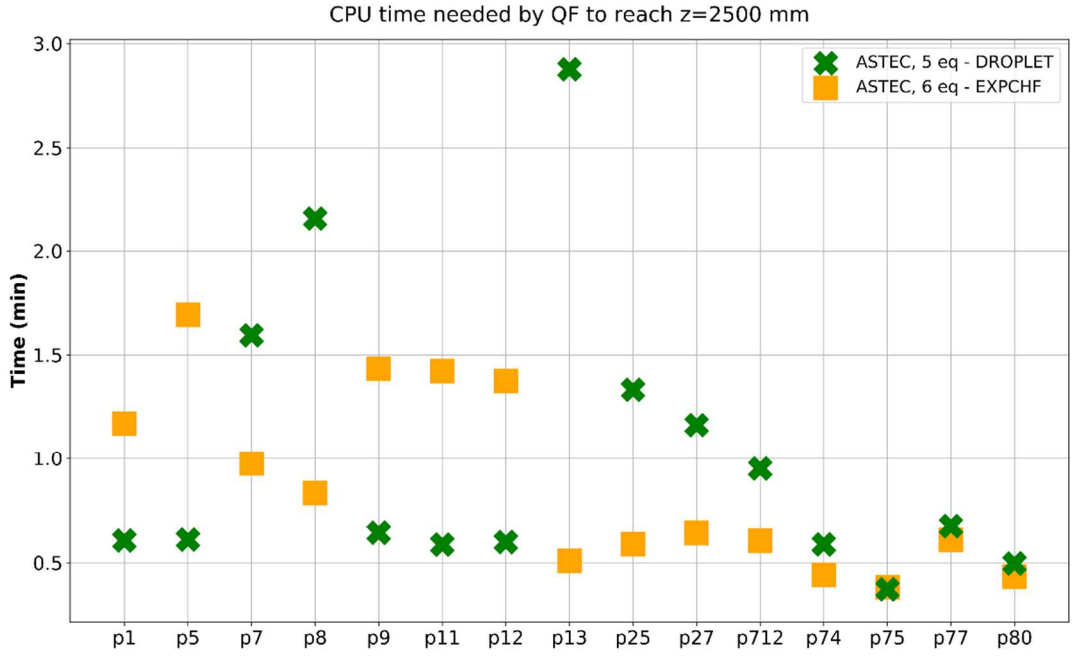


Figure 10: Computational times associated with the quenching of the rods up to 2500 mm for two most suitable modelling options of this study (DROPLET and CESAR five equations, EXPCHF and CESAR six-equations).

# 7 Conclusions

Within this article, the reference reflooding model of ASTEC V2.1, devoted to bottom flooding, has been alternately used with the five and six-equation schemes to simulate experiments of intact core reflooding performed in the PERICLES test facility. While the five-equation scheme uses a differential equation on the mean velocity and algebraic equation to calculate the drift velocity, the later solves two differential equations on the phase velocities with implicit appearance of the interfacial friction. The reference reflooding model is based on two main assumptions:

- A quench front is calculated if the temperature of a solid heated component falls below $T_{sat}$+5 and if the temperature of its upper component neighbour exceeds $T_{MFB}$, providing there is enough water in the mesh.
- The heat transfer along the vicinity of the quench front is the sum of two contributions. First, an exponentially decreasing function over an empirical length, this approach being taken from (Chikhi and Fichot, 2010; Nelson and Unal, 1992). Second, the existence of a large and uniform heat transfer coefficient over a longer distance, this representing the projection of droplets well above the front. They are named EXPCHF and DROPLET model, respectively.

Calculations using different combinations of hydrodynamic models and heat transfer reflooding models along the TBR have been performed. The main conclusion is that the choice of the reflooding model depends on the choice of the hydrodynamic model. If the five-equation scheme is selected, the DROPLET model is the most appropriate option. However, if the six-equation scheme is used, the EXPCHF model is best, since it benefits from the larger amount of liquid available near the front. Computational costs are not significantly impaired by using either option, but reactor calculations should be carried out to give more validity to this statement.

In turn, the present article recommends the using the six-equation approach together with the EXPCHF model for accidental sequences involving reflooding, because of the more significant physical soundness of the system together with improved validation results on PERICLES experiments.

There are still developments that can be put in place to improve the modelling in both situations. Concerning the modelling in six-equations, improvements in the description of the Critical Heat Flux could be developed and additional terms can be introduced in the $L_l$ length as suggested by (Nelson and Unal, 1992). With regards to the five-equation scheme, it makes sense to replace the fixed TBR length ($Z_D$) by a dynamic length that depends on the capillary number and a multiplicative factor, to avoid excessive precooling far above the front.

# References

Berenson, P., 1961. Film boiling heat transfer from an horizontal surface. J. Heat Transfer 83, 351–358.

https://doi.org/doi:10.1115/1.3682280

Bestion, D., 2011. System Code Models and Capabilities, in: THICKET 2008 – Session III. Pisa, Italy, May 5–9, pp. 81–106.

Broughton, J.M., Kuan, P., Petti, D.A., Tolman, E.L., 1989. A Scenario of the Three Mile Island Unit 2 Accident. Nucl. Technol. 87, 34–53. https://doi.org/10.13182/NT89-A27637

Chatelard, P., Belon, S., Bosland, L., Carénini, L., Coindreau, O., Cousin, F., Marchetto, C., Nowack, H., Piar, L., Chailan, L., 2016. Main modelling features of the ASTEC V2.1 major version. Ann. Nucl. Energy 93, 83–93. https://doi.org/10.1016/j.anucene.2015.12.026

Chatelard, P., Reinke, N., Arndt, S., Belon, S., Cantrel, L., Carenini, L., Chevalier-Jabet, K., Cousin, F., Eckel, J., Jacq, F., Marchetto, C., Mun, C., Piar, L., 2014. ASTEC V2 severe accident integral code main features, current V2.0 modelling status, perspectives. Nucl. Eng. Des. 272, 119–135. https://doi.org/10.1016/j.nucengdes.2013.06.040

Chikhi, N., Fichot, F., 2010. Reflooding model for quasi-intact rod configuration: Quench front tracking and heat transfer closure laws. Nucl. Eng. Des. 240, 3387–3396. https://doi.org/10.1016/j.nucengdes.2010.07.011

Chikhi, N., Fleurot, J., 2012. Revisiting the QUENCH-11 integral reflood test with a new thermal-hydraulic model: Existence of a minimum injection rate. Ann. Nucl. Energy 49, 12–22. https://doi.org/10.1016/j.anucene.2012.06.004

Chikhi, N., Nguyen, N.G., Fleurot, J., 2012. Determination of the hydrogen source term during the reflooding of an overheated core: Calculation results of the integral reflood test QUENCH-03 with PWR-type bundle. Nucl. Eng. Des. 250, 351–363. https://doi.org/10.1016/j.nucengdes.2012.05.026

Cronenberg, A.W., 1992. Hydrogen generation behaviour in the LOFT FP-2 and other experiments: comparative assessment for migrated severe accident conditions. Nucl. Technol. 97, 91–112. https://doi.org/10.13182/NT92-A34629

Digonnet, A., Veteau, J.M., 1989. PERICLES Programme : boil-up, boil-off and reflooding high pressure experiments in a PWR assembly, in: Proceedings of the European Two-Phase Flow Group Meeting. Paris, France.

Digonnet, A., Veteau, J.M., Blanc, J.P., Lambert, M., 1988. Essais de renoyage d'un assemblage complet de réacteur à eau pressurisée - Essais bouillotte et de dénoyage Essais transitoires mixtes. Note SETh/LES/88-54 (Internal report). Grenoble, France.

Glantz, T., Taurines, T., Belon, S., De Luze, O., Guillard, G., Jacq, F., 2018. DRACCAR: A multi-physics code for computational analysis of multi-rod ballooning, coolability and fuel relocation during LOCA transients. Part One: General modeling description. Nucl. Eng. Des. 339, 202–214. https://doi.org/10.1016/j.nucengdes.2018.08.031

Gómez-García-Toraño, I., Laborde, L., 2019. Validation of the CESAR friction models of the ASTECV21 code based on Moby Dick experiments. J. Nucl. Eng. Radiat. Sci. 5, 1–9. https://doi.org/DOI: 10.1115/1.4042119

Hering, W., Homann, C., 2007. Degraded core reflood: Present understanding and impact on LWRs. Nucl. Eng. Des. 237, 2315–2321. https://doi.org/10.1016/j.nucengdes.2007.04.017

Hering, W., Homann, C., Stuckert, J., 2015. Integration of New Experiments into the Reflood Map, in: Proceedings of the 15th International Congress on Advances in Nuclear Power Plants (ICAPP-15). pp. 1420–1428. https://doi.org/10.5445/IR/170100914

Hermsmeyer, S., Iglesias, R., Herranz, L.E., Reer, B., Sangiorgi, M., 2014. Review of current Severe Accident Management ( SAM ) approaches for Nuclear Power Plants in Europe requirements. https://doi.org/10.2790/38824

Hochreiter, L.E., Cheung, F.B., Lin, T.F., Spring, J.P., Ergun, S., Sridharan, A., Ireland, A., Rosa, E.R., 2012. RBHT Reflood Heat Transfer Experiments Data and Analysis (NUREG/CR-6980).

Housiadas, C., Veteau, J.M., Deruaz, R., 1989. Two-dimensional quench front progression in a multi-assembly rod bundle. Nucl. Eng. Des. 113, 87–98. https://doi.org/https://doi.org/10.1016/0029-

5493(89)90299-9.

Humphries, L.L., Beeny, B.A., Gelbard, F., Louie, D.L., Phillips, J., 2017. MELCOR Computer Code Manuals Vol. 2: Reference Manual Version 2.2.9541. Albuquerque.

Ihle, P., Rust, K., 1984. FEBA - Flooding Experiments with Blocked Arrays Evaluation Report (KfK 3657). Karlsruhe. https://doi.org/10.5445/IR/270019863

Ishii, M., De Jarlais, G., 1987. Flow visualization study of inverted annular flow of post dryout heat transfer region. Nucl. Eng. Des. 99, 187–199. https://doi.org/10.1016/0029-5493(87)90120-8

Ivey, H., Morris, D., 1962. On the relevance of the vapour-liquid exchange mechanism for subcooled boiling heat transfer at high pressure. Reactor Development Division, Atomic Energy Establishment, Dorset, England.

Lee, N., Wong, S., Yeh, H.C., Hochreiter, L.E., 1982. PWR FLECHT SEASET unblocked bundle, forced and gravity reflood task data evaluation and analysis report (EPRI-NP-2013). Monroeville, Pennsylvania.

Mendizábal, R., Alfonso, E. de, Freixa, J., Reventós, F., 2017. Post-BEMUSE Reflood Model Input Uncertainty Methods (PREMIUM) Benchmark: Final Report (NEA-CSNI-R--2016-18). Nuclear Energy Agency of the OECD (NEA).

NEA-OECD, 2010. Core Exit Temperature (CET) Effectiveness in Accident Management of Nuclear Power Reactor. NEA/CSNI/R9.

Nelson, R., Unal, C., 1992. A phenomenological model of the thermal hydraulics of convective boiling during the quenching of hot rod bundles Part I: Thermal hydraulic model. Nucl. Eng. Des. 136, 277–298. https://doi.org/10.1016/0029-5493(92)90029-U

Obot, N.T., Ishii, M., 1988. Two-phase flow regime transition criteria in post-dryout region based on flow visualization experiments. Int. J. Heat Mass Transf. 31, 2559–2570. https://doi.org/10.1016/0017-9310(88)90182-2

Schanz, G., Hagen, S., Hofmann, P., Schumacher, G., Sepold, L., 1992. Information on the evolution of severe LWR fuel element damage obtained in the CORA program. J. Nucl. Mater. 188, 131–145. https://doi.org/10.1016/0022-3115(92)90462-T

Sepold, L., Hofmann, P., Leiling, W., Miassoedov, A., Piel, D., Schmidt, L., Steinbru, M., 2001. Reflooding experiments with LWR-type fuel rod simulators in the QUENCH facility. Nucl. Eng. Des. 204, 205–220. https://doi.org/https://doi.org/10.1016/S0029-5493(00)00308-3

Steinbrück, M., Große, M., Sepold, L., Stuckert, J., 2010. Synopsis and outcome of the QUENCH experimental program. Nucl. Eng. Des. 240, 1714–1727. https://doi.org/10.1016/j.nucengdes.2010.03.021

Thom, J.R.S., Walker, W.M., Fallon, T.A., Reising, G.F.S., 1965. Boiling in Sub-Cooled Water during Flow up Heated Tubes or Annuli, in: Symposium on Boiling Heat Transfer in Steam Generation Units and Heat Exchangers. pp. 226–246. https://doi.org/10.1243/pime_conf_1965_180_117_02

Wallis, G., 1969. One-Dimensional Two Phase Flow. McGraw-Hill, New York.

Yadigaroglu, G., Nelson, R.A., Teschendorff, V., Murao, Y., Kelly, J., Bestion, D., 1993. Modeling of reflooding. Nucl. Eng. Des. 145, 1–35. https://doi.org/10.1016/0029-5493(93)90056-F